Materials Chemistry and Physics 182 (2016) 182–189

Contents lists available at ScienceDirect

Materials Chemistry and Physics

journal homepage: www.elsevier.com/locate/matchemphys

First-principles investigation of the optical properties for rocksalt mixed metal oxide $Mg_xZn_{1-x}O$

Moufdi Hadjab [a, b], Smail Berrah [c], Hamza Abid [a], Mohamed Issam Ziane [a], Hamza Bennacer [a], Ali H. Reshak [d, e, *]

[a] Applied Materials Laboratory, Research Center, University Djillali Liabes, 22000, Sidi Bel Abbes, Algeria
[b] Thin Films Development and Applications Unit UDCMA, Setif – Research Center in Industrial Technologies CRTI, P. O. Box 64, Cheraga, 16014, Algiers, Algeria
[c] Mastery Renewable Energies Laboratory (LMER), University of A. Mira, Bejaia, Algeria
[d] New Technologies – Research Center, University of West Bohemia, Univerzitni 8, 30614, Pilsen, Czech Republic
[e] Center of Excellence Geopolymer and Green Technology, School of Material Engineering, University Malaysia Perlis, 01007, Kangar, Perlis, Malaysia

HIGHLIGHTS

- Theoretical study of optical properties of the cubic alloy $Mg_xZn_{1-x}O$.
- The lattice constants, the bulk modulus B and it's pressure derivative B′ were obtained.
- The calculated energy gaps within mBJ show good agreement with the experimental data.
- The optical properties were calculated and discussed in details.

GRAPHICAL ABSTRACT

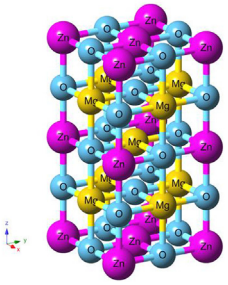

ARTICLE INFO

Article history:
Received 26 October 2015
Received in revised form
30 May 2016
Accepted 9 July 2016
Available online 16 July 2016

Keywords:
Alloys
Electronic materials
Optical materials
Ab initio calculations
Band-structure

ABSTRACT

In this paper, we have presented a theoretical study of the optical properties for the cubic $Mg_xZn_{1-x}O$ (x = 0.0, 0.125, 0.375, 0.625, 0.875 and 1.0) alloys using the full-potential linearized augmented plane wave (FP-LAPW) method based on the density functional theory (DFT). The local density approximation (LDA) was applied to calculate the structural properties. In order to explore the desired properties, the $Mg_xZn_{1-x}O$ alloys were modeled at various x compositions from 0.0 to 1.0 by step of 0.125. The recently modified semi-local Becke-Johnson potential with LDA correlation in the form of mBJ-LDA was used to predict the energy band gap, optical dielectric function, refractive index, absorption coefficient, reflectivity, optical conductivity and the electron energy loss of $Mg_xZn_{1-x}O$ alloys. The obtained results show good agreement with the experimental data, which indicate that the investigated ternary alloys are among promising material for the fabrication of electronic, optoelectronic devices and their applications.

1. Introduction

In recent years, group II-VI semiconductor materials, such as ZnO, MgO and their ternary alloy $Mg_xZn_{1-x}O$, have drawn considerable attention, which have become an important part of our life.

* Corresponding author. New Technologies – Research Center, University of West Bohemia, Univerzitni 8, 30614, Pilsen, Czech Republic.
E-mail address: maalidph@yahoo.co.uk (A.H. Reshak).

http://dx.doi.org/10.1016/j.matchemphys.2016.07.021
0254-0584/

These semiconductor compounds have a versatile applications in modern electronic, owing to their high photoconductivity, large piezoelectric coefficient, transparency in the wavelength regimes and wide band-gap range from around 3.4 eV–7.8 eV, for wurtzite ZnO and rocksalt MgO, respectively [1–3]. These materials have been used in a good number of optoelectronic devices, frequently employed for catalytic applications [4], solar-blind responsivity of photodetectors [5], magnetic tunnel junction for information storage [2], ultraviolet photoconductive detector [6], high-density optical memories, visual displays, transparent conductors, laser and piezoelectric devices, gas sensors, varistors and thin films solar cells, etc. [7,8].

Some theoretical investigations reported that the mixed metal oxide are found in the rocksalt structure [9,10]. Aoumeur et al. [9] and Amrani et al. [10], have calculated the structural and electronic properties of $Mg_xZn_{1-x}O$ alloy using the Full-Potential Linear-Muffin-Tin-Orbital (FP-LMTO) method. The structural, electronic and thermodynamic properties of $Mg_xZn_{1-x}O$ alloys are also studied by using the full-potential linearized augmented plane wave (FP-LAPW) within Perdew–Burke–Ernzerhof generalized gradient approximation (PBE-GGA) [11] and the improved form by Engel and Vosko (EV-GGA) [12]. Finally, Fritsh et al. [13] have investigated the electronic properties of $Mg_xZn_{1-x}O$ by means of the Empirical Pseudopotential Method (EPM). To the best of our knowledge, there is no other theoretical investigation on the electronic and optical properties of the ternary (Mg,Zn)O alloy using (FP-LAPW) method, within the recently modified semi-local Becke–Johnson potential (mBJ) [14]. In the light of the importance of these alloys in various optoelectronic applications, our aim in this paper was drawn to investigate the optical properties of $Mg_xZn_{1-x}O$ alloys in the rocksalt structure.

The paper is organized as follows; in section two, we present the computational method. The results and discussions of the structural, electronic and optical properties are shown in section three. Finally, the conclusion of our work is presented in section four.

2. Computational details

Total energy calculations of the optoelectronic properties of the cubic $Mg_xZn_{1-x}O$ for x vary between 0.0 and 1.0 with a pitch of 0.125, has been performed using the full-potential linearized augmented plane wave (FP-LAPW) method as implemented in Wien2k computational code [15]. In this method, the unit cell is partitioned into non-overlapping Muffin-Tin spheres around the atomic sites and the interstitial region, a use of different basis sets is possible for these two types of regions, the Kohn-Sham equation which is based on the density functional theory (DFT) [16,17] is solved according to a self consistent scheme. For the exchange-correlation potential, the local density approximation (LDA) [18,19] was applied only for calculating the structural properties. Since standard semi-local functionals, such as LDA or GGA, underestimate the band gaps therefore, we proposed to use the modified Becke-Johnson (mBJ) potential [14]. This method is a modified version of the Becke-Johnson potential used to improve band gaps obtained by the conventional DFT-based methods, mBJ allows the calculation of band gaps with accuracy similar to the very expensive GW calculations. The mBJ potential can be written as:

$$\upsilon_{x,\sigma}^{mBJ}\left(\vec{r}\right) = c\upsilon_{x,\sigma}^{BR}\left(\vec{r}\right) + (3c-2)\frac{1}{\pi}\sqrt{\frac{5}{6}}\sqrt{\frac{\tau_\sigma\left(\vec{r}\right)}{\rho_\sigma\left(\vec{r}\right)}} \quad (1)$$

where ρ_σ is the electron density, τ_σ is the kinetic-energy and $\upsilon_{x,\sigma}^{BR}$ is the Becke-Roussel potential [20]. The c parameter is a system-dependent parameter, with $c = 1$ corresponding to the original Becke-Johnson potential. For bulk crystalline materials, Tran and Blaha proposed to determine c by the following empirical relation:

$$c = \alpha + \beta\left(\frac{1}{V_{cell}}\int_{cell}\frac{\left|\nabla\rho_\sigma(r')\right|}{\rho_\sigma(r')}d^3r'\right)^{\frac{1}{2}} \quad (2)$$

where V_{cell} means the unit cell volume, $\alpha = -0.012$ and $\beta = 1.023$ bohr$^{1/2}$ are parameters fitted according to experimental values [14]. Using this modified Becke-Johnson potential, the band gaps of many insulating systems can be described accurately with an effort that is in general comparable to that of LDA/GGA [14,21,22]. For electronic structure calculations, the modified Becke-Johnson exchange potential is used due to significantly improved band gap results. The mBJ exchange correlation potential as an orbital independent, semi-local exchange correlation potential has been proved to produce accurate gaps for wide band gap insulators, sp semiconductors, 3d transition-metal oxides [14,23] half-metallicity [24,25] and doped semiconductors systems [26–28].

To get energy eigenvalues convergence, the plane wave expansion with an $R_{MT} \times K_{MAX}$ was chosen to be equal to 8, where R_{MT} is the smallest radii of the Muffin-Tin spheres and K_{MAX} is the cut-off for the wave function basis. The R_{MT} values (Muffin-Tin radii) were taken to be 1.85, 2.05 and 1.7 atomic unit (a.u) for Mg, Zn and O, respectively, for our binary and ternary compounds. The spherical harmonics inside non-overlapping Muffin-Tin (MT) spheres surrounding the atoms are expanded up to $l_{max} = 10$. The Fourier-expanded charge density was truncated at $G_{max} = 12$ (a.u)$^{-1}$. In this work, a 16 atoms simple cubic supercell which corresponds to $1 \times 1 \times 2$ conventional cell was used to simulate the $Mg_xZn_{1-x}O$ alloys (Fig. 1). The geometric arrangements are summarized in Table 1. The irreducible wedge of the Brillouin zone (BZ) was described by a mesh of 108 special **k**-points (grid of $10 \times 10 \times 5$ meshes, equivalent to 500 K-points in the entire BZ). In the optical

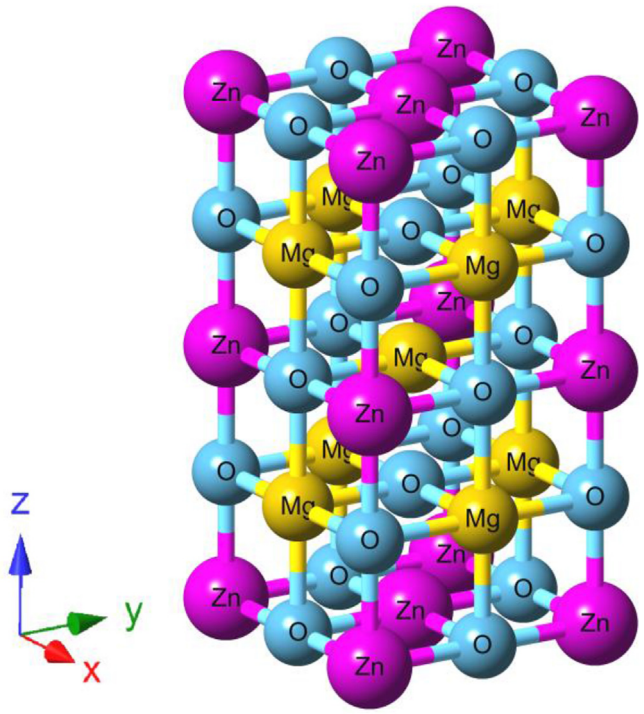

Fig. 1. Crystal structure of $Mg_{0.625}Zn_{0.375}O$ (supercell).

Table 1
The relaxed Mg atomic positions in $Mg_xZn_{1-x}O$ (x = 0.125, 0.375, 0.625 and 0.875) alloys.

Material	Mg atom positions (x, y, z)
$Mg_{0.125}Zn_{0.875}O$	Mg_1(0.5, 0.5, 0.5)
$Mg_{0.25}Zn_{0.75}O$	Mg_1(0.5, 0.5, 0.5011), Mg_2(0.5, 0.0, 0.2488)
$Mg_{0.375}Zn_{0.625}O$	Mg_1(0.5, 0.5, 0.5), Mg_2(0.5, 0.0, 0.249), Mg_3(0.5, 0.0, 0.7509)
$Mg_{0.5}Zn_{0.5}O$	Mg_1(0.5, 0.5, 0.5007), Mg_2(0.5, 0.0, 0.2495), Mg_3(0.5, 0.0, 0.7511), Mg_4(0.0, 0.5, 0.2492)
$Mg_{0.625}Zn_{0.375}O$	Mg_1(0.5, 0.5, 0.5), Mg_2(0.5, 0.0, 0.2494), Mg_3(0.5, 0.0, 0.7505), Mg_4(0.0, 0.5, 0.2494), Mg_5(0.0, 0.5, 0.7505)
$Mg_{0.75}Zn_{0.25}O$	Mg_1(0.5, 0.5, 0.0), Mg_2(0.5, 0.5, 0. 5), Mg_3(0.5, 0.0, 0.25), Mg_4(0.5, 0.0, 0.75), Mg_5(0.0, 0.5, 0.25), Mg_6(0.0, 0.5, 0.75)
$Mg_{0.875}Zn_{0.125}O$	Mg_1(0.0, 0.0, 0.5), Mg_2(0.5, 0.5, 0.0), Mg_3(0.5, 0.5, 0.5), Mg_4(0.5, 0.0, 0.2496), Mg_5(0.5, 0.0, 0.7503), Mg_6(0.0, 0.5, 0.2496), Mg_7(0.0, 0.5, 0.7503)

calculations part, we have used denser meshes presented by 196 **k**-points. Self-consistent calculations are considered to be converged when the total energy of the system is stable within 10^{-5} Ryd.

3. Results and discussion

3.1. Structural properties

The calculations were firstly carried out to determine the structural properties of the binary and ternary alloys $Mg_xZn_{1-x}O$ (x = 0.0, 0.125, 0.25, 0.375, 0.5, 0.625, 0.75, 0.875 and 1.0.) with its cubic structure crystalline. In order to gain deep insight into the physical properties, we have performed volume optimization by using the experimental values for binary compounds as of entered parameters. The relaxed equilibrium structural parameters; the calculated lattice constant, bulk modulus and its pressure derivative, were obtained by fitting the total energy versus volume to Murnaghan's equation of states (EOS) [29]. The obtained structural values are listed in Table 2 in comparison to the experimental data [30,37] and the previous theoretical calculations using FP-LMTO method [9] and the FP-LAPW [10] within PBE-GGA. It is clear that our calculated results agree well with the experimental and theoretical values. Nevertheless, we have noticed that LDA underestimate the lattice parameters by around 1.19%–1.25% compared to the experimental data. It should be also noted the values of the bulk modulus decreases with increasing Mg content as seen from Table 2. This result represents bond strengthening or weakening effect induced by changing the concentration.

3.2. Electronic properties

In this section, we have computed and plotted the band structures of (Mg,Zn)O alloys along various high-symmetry directions in the first Brillouin zone (BZ) as shown in Fig. 2. Table 3 shows the calculated band gaps performed with and without relaxation effects for all studied concentrations (x = 0.0, 0.125, 0.25, 0.375, 0.5, 0.625, 0.75, 0.875, 1.0) in order to understand the changeability between relaxed and un-relaxed ternary structures. The calculated electronic band structure reveals that the $Mg_xZn_{1-x}O$ alloys possess indirect band gap (Γ-M) for x = 0.0, 0.125, 0.25, 0.375, 0.5, 0.625, 0.75, 0.875 while for x = 1.0 the band gap is a direct one (Γ-Γ) which agree well with the experiment [44,45] and other theoretical calculation [9].

In addition, we calculated the total bowing parameter b by fitting the non-linear variation of the computed band gaps versus concentration using the quadratic semi-empirical function:

$$E_{g(Mg_xZn_{1-x}O)}(x) = xE_{g(MgO)} + (1-x)E_{g(ZnO)} - x(1-x)b \quad (3)$$

Table 2
Calculated lattice constant a, bulk modulus B and it's pressure derivative B′ according to LDA approximation for ZnO, MgO and $Mg_xZn_{1-x}O$, in comparison with experimental and other theoretical calculations.

Material	a (Å)			B (GPa)			B'	
	LDA	Exp.	Theoretical results	LDA	Exp.	Theoretical results	LDA	Theoretical results
ZnO	4.22	4.271[a]	4.228[b], 4.223[c], 4.211[d], 4.213[e], 4.22[f], 4.337[g], 4.261[h]	209.00	202.5[i]	203.3[i], 198.02[f], 166.649[g]	4.78	4.23[f]
$Zn_{0.125}Mg_{0.875}O$	4.21			204.40			4.73	
$Zn_{0.25}Mg_{0.75}O$	4.21		4.208[f], 4.316[g]	199.92		190.032[f], 161.479[g]	4.58	4.29[f]
$Zn_{0.375}Mg_{0.625}O$	4.20			195.36			4.61	
$Zn_{0.5}Mg_{0.5}O$	4.19		4.196[f], 4.298[g]	190.85		186.628[f], 157.204[g]	4.48	4.39[f]
$Zn_{0.625}Mg_{0.375}O$	4.19			186.23			4.49	
$Zn_{0.75}Mg_{0.25}O$	4.18		4.185[f], 4.279[g]	181.73		179.08[f], 153.312[g]	4.41	4.36[f]
$Zn_{0.875}Mg_{0.125}O$	4.17			177.05			4.34	
MgO	4.16	4.213[k], 4.203[l], 4.212[m]	4.16[b,n], 4.247[b], 4.259[o], 4.173[f], 4.261[g], 4.237[h]	172.46	168.8[p], 156[q]	175.06[f], 161.9[g]	4.28	4.02[f]

[a] Ref [30].
[b] Ref [31].
[c] Ref [32].
[d] Ref [7].
[e] Ref [33].
[f] Ref [9].
[g] Ref [10].
[h] Ref [34].
[i] Ref [35].
[j] Ref [36].
[k] Ref [37].
[l] Ref [38].
[m] Ref [39].
[n] Ref [40].
[o] Ref [41].
[p] Ref [42].
[q] Ref [43].

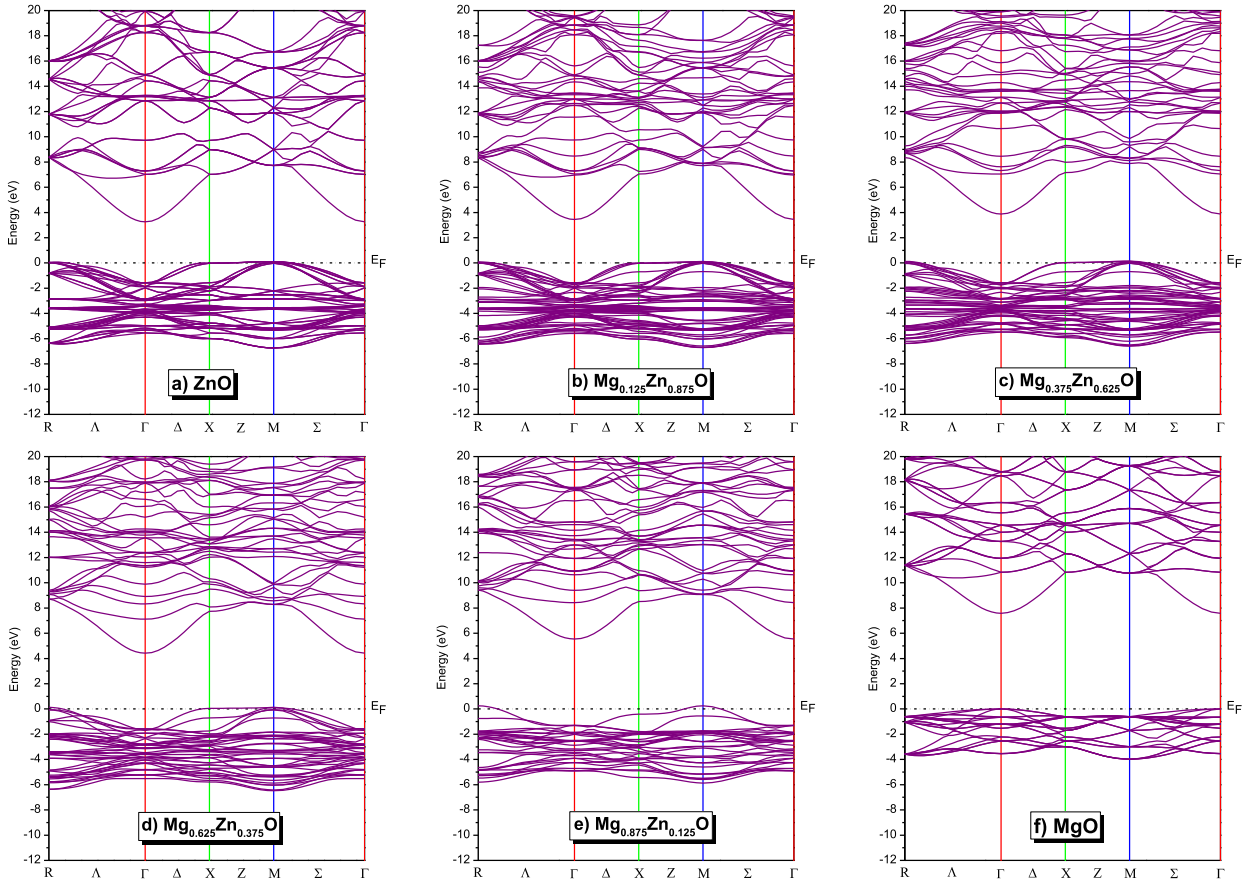

Fig. 2. Relaxed band structure of $Mg_xZn_{1-x}O$ alloys at the equilibrium lattice constant, for a($x = 0.0$), b($x = 0.125$), c($x = 0.375$), d($x = 0.625$), e($x = 0.875$) and f($x = 1.0$), using mBJ-LDA functional.

Table 3
Calculated values of the indirect and direct band gap of $Mg_xZn_{1-x}O$ alloys obtained within mBJ-LDA approximation in comparsion with experimental data and other theoretical values.

Material	Eg (eV)			
	mBJ-LDA		Exp.	Theoretical results
	Unrelaxed	Relaxed		
ZnO	3.16 (M -Γ)	3.16 (M-Γ)	2.7[a]	1.1[b], 1.27[c], 1.196[d], 1.466[e]
$Zn_{0.125}Mg_{0.875}O$	3.34 (M-Γ)	3.33 (M-Γ)	–	–
$Zn_{0.25}Mg_{0.75}O$	3.57 (M-Γ)	3.55 (M-Γ)	–	1.644[d]
$Zn_{0.375}Mg_{0.625}O$	3.75 (M-Γ)	3.73 (M-Γ)	–	–
$Zn_{0.5}Mg_{0.5}O$	4.08 (M-Γ)	4.02 (M-Γ)	–	2.069[d]
$Zn_{0.625}Mg_{0.375}O$	4.34 (M-Γ)	4.29 (M-Γ)	–	–
$Zn_{0.75}Mg_{0.25}O$	4.67 (M-Γ)	4.67 (M-Γ)	–	2.581[d]
$Zn_{0.875}Mg_{0.125}O$	5.25 (M-Γ)	5.28 (M-Γ)	–	–
MgO	7.58 (Γ-Γ)	7.58 (Γ-Γ)	7.83[f]	5.05[g], 4.982[h], 4.766[d], 5.409[e]

[a] Ref. [44].
[b] Ref. [32].
[c] Ref. [7].
[d] Ref. [9].
[e] Ref. [10].
[f] Ref. [45].
[g] Ref. [46].
[h] Ref. [47].

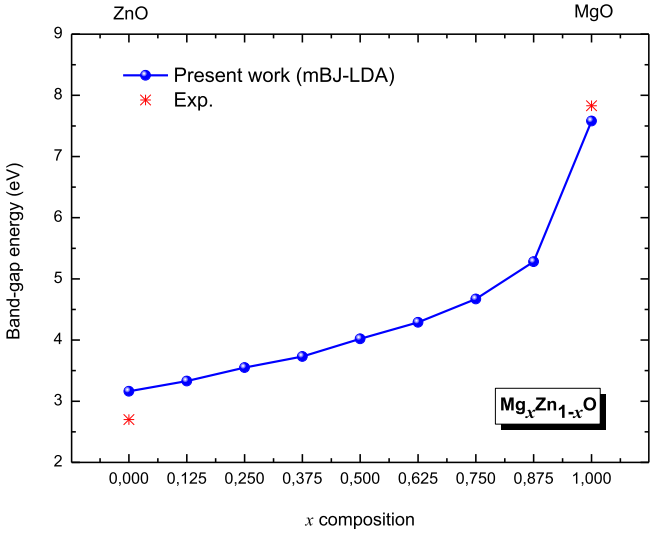

Fig. 3. Band gap as a function of Mg concentrations for relaxed $Mg_xZn_{1-x}O$ alloys using the mBJ-LDA, compared with experimental data [44,45].

This equation gives $b = 5.44$, according to the mBJ-LDA approximation. Our calculated band gap values for the relaxed $Mg_xZn_{1-x}O$ ternary alloys as shown in Fig. 3 are fitted by the expression (3), and follow the quadratic eq. (4):

$$Eg^{mBJ-LDA}_{Mg_xZn_{1-x}O} = 3.44 - 1.93x + 5.44x^2 \quad (4)$$

The non-linear behaviour are found for the variations of our calculated band gap values versus the composition x. This

behaviour was also observed by Aoumeur et al. [9] using FP-LMTO calculations and Amrani et al. [10] using FP-LAPW method within EV-GGA.

3.3. Optical properties

In this part, we present the optical dielectric function, optical conductivity, refractive index, reflectivity, absorption coefficient and the electron energy loss of the cubic binary ZnO, MgO and their ternary alloys $Mg_xZn_{1-x}O$. The optical properties are considered as an important source of information concerning the electronic bands structures, it is usually deduced from the dielectric function that given by:

$$\varepsilon = \varepsilon_1(\omega) + i\varepsilon_2(\omega) \quad (5)$$

where ω is the angular frequency, $\varepsilon_1(\omega)$ and $\varepsilon_2(\omega)$ are the real and the imaginary components of the complex dielectric function, respectively. Hence, the imaginary part of the dielectric function $\varepsilon_2(\omega)$ is calculated from the momentum matrix elements between the occupied and unoccupied states and their wave functions. The real part of dielectric function, $\varepsilon_1(\omega)$, can be derived from $\varepsilon_2(\omega)$ by using the Kramer–Kroning relation [48,49]. From $\varepsilon_1(\omega)$ and $\varepsilon_2(\omega)$ components of the dielectric function we can derive other interesting quantities, such as absorption coefficient $\alpha(\omega)$, refractive index $n(\omega)$, extinction coefficient $k(\omega)$, optical conductivity $\kappa(\omega)$, reflectivity $R(\omega)$ and the electron energy loss function $L(\omega)$. For calculating the optical properties, a dense mesh of uniformly distributed **k**-points is needed. Thus, the Brillouin zone (BZ) integration was achieved with 196 **k**-points in the irreducible part of the BZ, (grid of 12 × 12 × 6 meshes, equivalent to 1000 **k**-points). In this work we present the results obtained within mBJ-LDA approximation. The half-width broadening is taken to be 0.2 eV.

3.3.1. The real dielectric function

For ZnO, $\varepsilon_1(\omega)$ is positive up to 16.85 eV and presents several peaks located at 5.15 eV, 9.81 eV, 13.97 eV, and 16.45 eV. Also for MgO, it is positive up to 19.56 eV and has peaked three peaks at 11.2 eV, 13.26 eV and 17.0 eV. For $Mg_xZn_{1-x}O$, the $\varepsilon_1(\omega)$ has positive values up to 16.79 eV, 17.44 eV, 17.87 and 19.31 eV for $x = 0.125$, 0.375, 0.625 and 0.875, respectively. After that, $\varepsilon_1(\omega)$ becomes negative. It is clear that increasing the content of Mg cause to shift the peaks towards higher energies. Furthermore, our obtained values of the static dielectric constant $\varepsilon_1(0)$ are given in Table 4. It has been found that the calculated values of $\varepsilon_1(0)$ decreases with increasing composition x, for ($0 \le x \le 1$) and follow Penn model [50]. Penn proposed that $\varepsilon_1(0)$ is inversely proportional to the value of band gap (Fig. 4). The obtained mBJ-LDA results of $\varepsilon_1(\omega)$ for all concentrations x are shown in Fig. 5.

Table 4
Static refractive index, static reflectivity and optical dielectric constant of $Mg_xZn_{1-x}O$ alloys, obtained within mBJ-LDA approximation in comparsion with experimental data and other theoretical results.

Material	n(0)	R(0)	$\varepsilon_1(0)$
ZnO	1.81	0.08, 0.11[a]	3.27, 4.06[a]
$Zn_{0.125}Mg_{0.875}O$	1.77	0.08	3.15
$Zn_{0.375}Mg_{0.625}O$	1.71	0.07	2.93
$Zn_{0.625}Mg_{0.375}O$	1.64	0.06	2.69
$Zn_{0.875}Mg_{0.125}O$	1.57	0.05	2.46
MgO	1.53	0.04	2.34, 2.94[b], 3.12[c]

[a] Ref. [53].
[b] Ref. [54].
[c] Ref. [55].

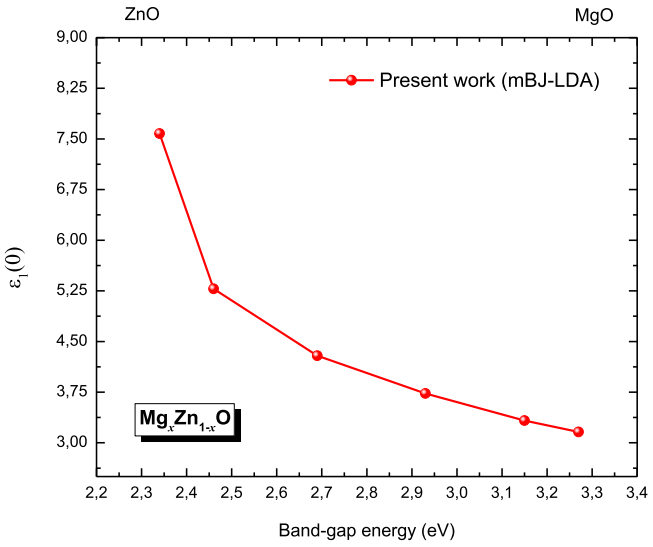

Fig. 4. Variation of the static dielectric constant with the band-gap values for relaxed $Mg_xZn_{1-x}O$ alloys, according to the Penn model.

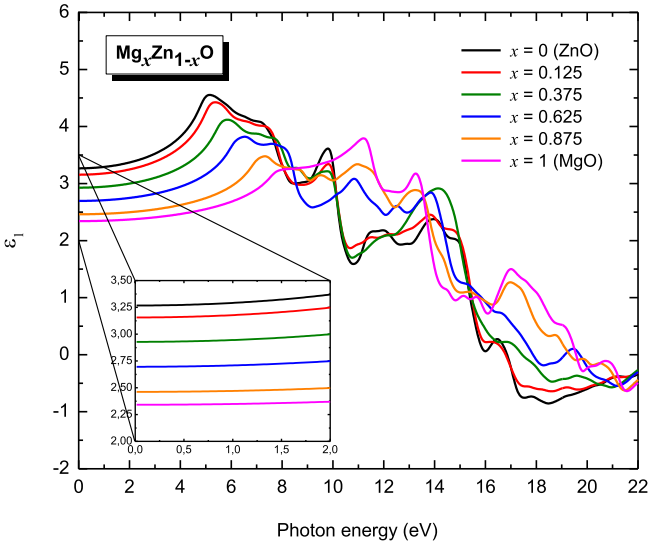

Fig. 5. Real part of the dielectric function for relaxed $Mg_xZn_{1-x}O$ alloys, within the modified Becke-Johnson approach (mBJ-LDA).

3.3.2. The imaginary dielectric function

The imaginary dielectric function is an important quantity; it shows the various interband transitions between the valence and conduction bands. From the feature of the imaginary part $\varepsilon_2(\omega)$ shown in Fig. 6, there are five groups of peaks, for ZnO and MgO, over a range of photon energies up to 25 eV. For ZnO, which have an indirect gap, the first peak is located at 3.16 eV which is mainly due to the optical transition (M_v–Γ_c). The first peak is followed by four other peaks corresponding to other interband transitions; these are located at 4.77, 7.85, 10.16 and 15.33 eV. While for MgO, The first peak situated at 7.47 eV stems from the direct optical transition (Γ_v–Γ_c), it followed by four other peaks located at 11.63, 13.75, 18.35 and 19.44 eV. For the ternary alloys $Mg_xZn_{1-x}O$ within the range $0.125 \le x \le 0.875$, the spectrum of the imaginary part $\varepsilon_2(\omega)$ is depicted in Fig. 7. For $x = 0.125$ is mostly dominated by the peaks of ZnO, but $x = 0.375$ is subjugated by a weak peaks of ZnO. For $x = 0.625$, we note the presence of the peaks of MgO, unless the

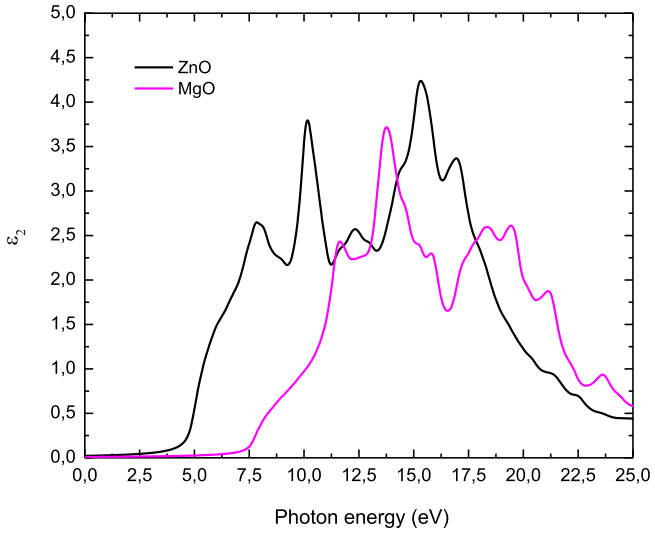

Fig. 6. Imaginary part of the dielectric function for relaxed ZnO and MgO compounds within the modified Becke-Johnson approach (mBJ-LDA).

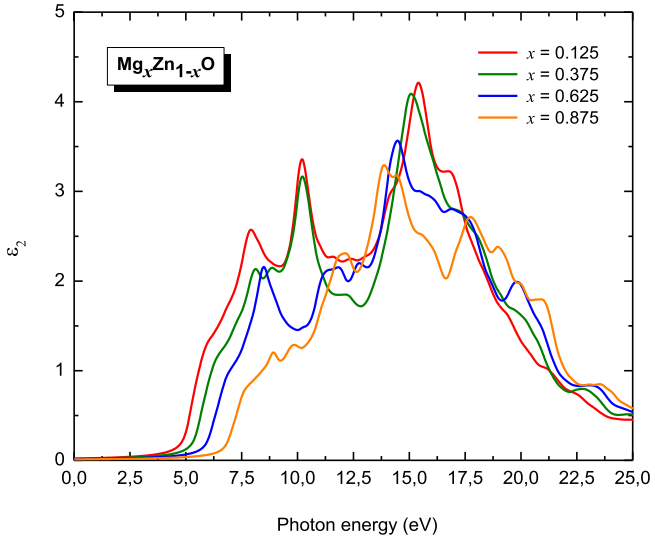

Fig. 7. Imaginary part of the dielectric function for relaxed $Mg_xZn_{1-x}O$ alloys within the modified Becke-Johnson approach (mBJ-LDA).

third peak which is derived from the third peak of ZnO. Finally, for $x = 0.875$, the peaks are generally conquered by the peaks of MgO.

3.3.3. Refractive index

The refractive index $n(\omega)$ is an essential optical parameter related to the microscopic atomic interaction [51]. It measures the transparency of semiconductor materials versus spectral radiations and has also an important role in the investigation of the opto-electronic properties. Furthermore, this parameter has indispensable impact for the devices such as detectors, solar cell and wave guides [52]. From the imaginary and real parts of the dielectric function we deduce the refractive index:

$$n(\omega) = \sqrt{\frac{\left(\varepsilon_1(\omega)^2 + \varepsilon_2(\omega)^2\right)^{1/2} + \varepsilon_1(\omega)}{2}} \quad (6)$$

The calculated refractive index of ternary alloys $Mg_xZn_{1-x}O$ within $0 \le x \le 1$ range, as a function of the photon energy, displayed in Fig. 8 indicates that there is shift towards lower values with increasing the content of Mg. The static refractive index for low frequency described by the relation $n(0) = \sqrt{\varepsilon_1}(0)$. These values are presented in Table 4.

3.3.4. Absorption coefficient

We have plotted the spectral components of the logarithmic absorption coefficient obtained within mBJ-LDA approximation in the energy range (0.0–22.0) eV for the binary compounds ZnO and MgO as shown in Fig. 9. It is clear that the binary compounds have an excellent optical absorption in a wide energy range (3.97–17.29) eV and (6.6–21.4) eV, which corresponds to wave length (71.7–312.3) nm and (57.93–187.85) nm for ZnO and MgO respectively. From the features of the optical absorption spectra (Fig. 9), the absorption edges of ZnO and MgO are located at 3.97 eV and 6.60 eV, respectively. Whereas the absorption edges of $Mg_xZn_{1-x}O$ ($x = 0.125$, 0.375, 0.625 and 0.875) are situated at 4.14, 4.54, 5.07 and 5.87 eV, respectively (see Fig. 10). For the alloy $Mg_xZn_{1-x}O$, the band gap is in this range [3.97–6.6] eV. It's obvious, from our calculation, the utility of these binary and ternary alloys for absorption purposes in the Ultraviolet (UV) region of the electromagnetic spectrum.

3.3.5. Optical conductivity

The plots of the optical conductivity $\kappa(\omega)$, within mBJ-LDA approximation are displayed in Figs. 11 and 12 over the range of photon energy up to 35 eV, for ZnO, MgO and their ternary alloys, respectively. The $\kappa(\omega)$ is deduced from the complex dielectric function (eq. (5)), which is given by:

$$\kappa(\omega) = \left(\frac{-i\omega}{4\pi}\right)\varepsilon(\omega) \quad (7)$$

Several peaks are presented in the feature of $\kappa(\omega)$ curves, which are vary in accordance with the energy band gap.

3.3.6. Reflectivity

Reflectivity $R(\omega)$ is one of the essential parameters in optical computations. In fact, reflectivity is sensitive to combination of the two parts of the dielectric function. Fig. 13 shows the reflectivity spectra of $Mg_xZn_{1-x}O$ for $0 \le x \le 1$ versus photon energy by using

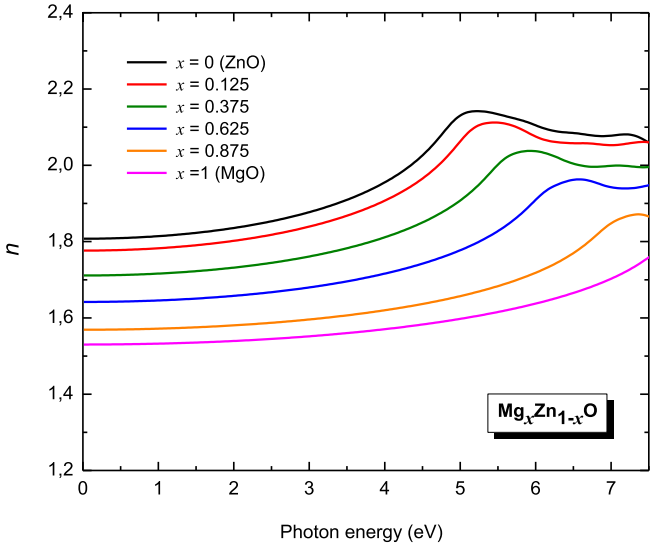

Fig. 8. Refractive index for relaxed $Mg_xZn_{1-x}O$ alloys within the modified Becke-Johnson approach (mBJ-LDA).

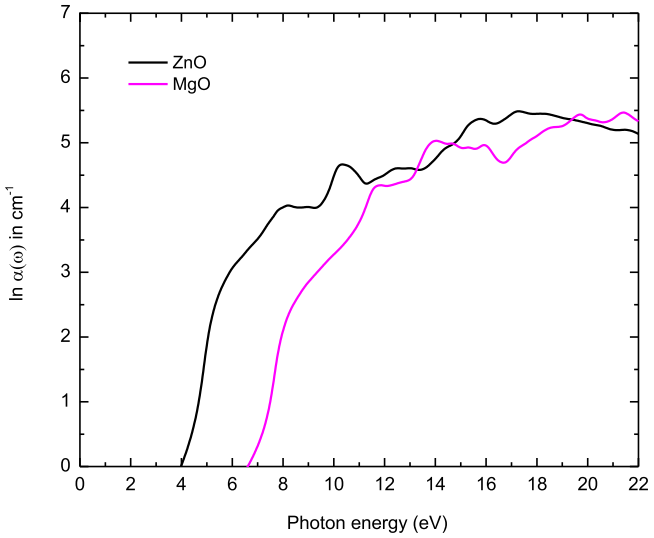

Fig. 9. Absorption function for relaxed ZnO and MgO compounds within the modified Becke-Johnson approach (mBJ-LDA).

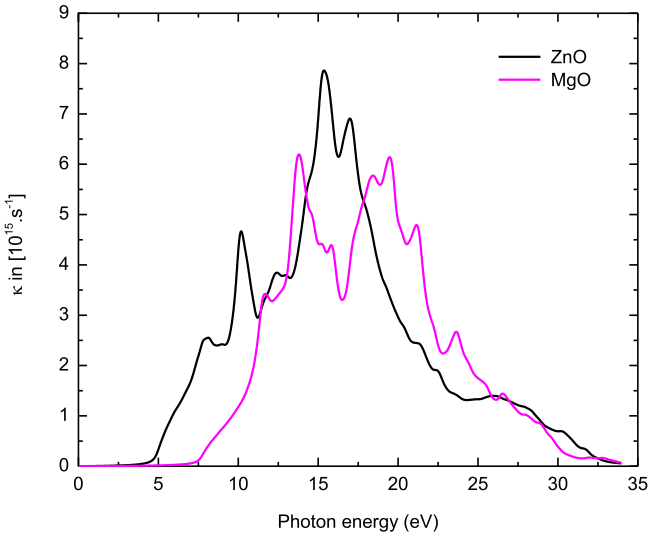

Fig. 11. Optical conductivity for relaxed ZnO and MgO compounds within the modified Becke-Johnson approach (mBJ-LDA).

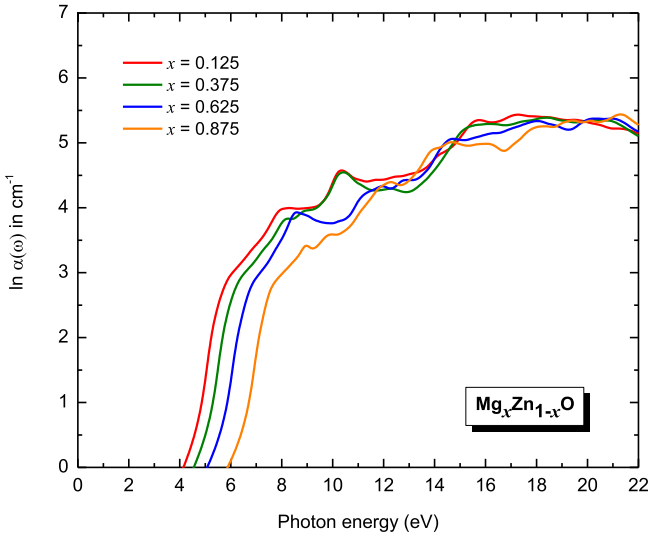

Fig. 10. Absorption function for relaxed $Mg_xZn_{1-x}O$ alloys within the modified Becke-Johnson approach (mBJ-LDA).

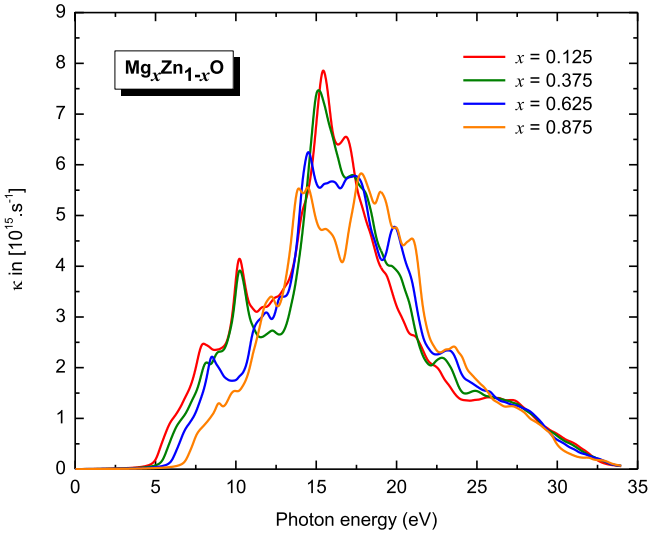

Fig. 12. Optical conductivity for relaxed $Mg_xZn_{1-x}O$ alloys within the modified Becke-Johnson approach (mBJ-LDA).

mBJ-LDA approximation. The zero frequency reflectivity $R(0)$ of the investigated materials are listed in Table 4. It is clear that increasing the Mg content lead to decrease the reflectivity at the static limit. The maximum values displayed in Fig. 13 are situated at 18.65, 19.87, 21.21, 21.4, 21.61 and 21.7 eV for $Mg_xZn_{1-x}O$ ($x = 0.0$, 0.125, 0.25, 0.375, 0.5, 0.625, 0.75, 0.875, 1.0), respectively. The wavelength of the maximum reflectivity is obtained around 0.057 μm (57.13 nm).

3.3.7. *Energy loss function (ELF)*

The electron energy-loss function spectra describe the energy loss of a fast crossing electron in materials. This function has the usefulness of enveloping the full energy range, involving scattered elastically and non-scattered electrons, which excite the electrons of the valence interband transitions or atom's outer shell [48]. It can be calculated by the following relation [56]:

$$L(\omega) = -\mathrm{Im}\left(\varepsilon^{-1}\right) = \frac{\varepsilon_1}{\varepsilon_1^2 + \varepsilon_2^2} \tag{8}$$

Fig. 14 illustrated the energy loss function of ZnO, MgO and their ternary alloys. The maximum critical point are located at 28.88, 28.74, 28.96, 29.15, 28.28 and 29.18 eV for $Mg_xZn_{1-x}O$ ($x = 0.0$, 0.125, 0.25, 0.375, 0.5, 0.625, 0.75, 0.875, 1.0), respectively. These points represent the lossless regions.

4. Conclusion

The purpose of this work is to study the optical properties of the cubic mixed metal oxide $Mg_xZn_{1-x}O$ for x vary between 0.0 and 1.0 by step of 0.125. We have used the all-electron FP-LAPW method within LDA for optimizing the lattice constants, the related bulk modulus B and it's pressure derivative B'. The obtained results show good agreement with the experimental data. To calculate the energy band gap we have used the recently modified semi-local Becke–Johnson potential (mBJ-LDA), we found that this approach brings the calculated energy gaps close to the experimental values and much better than the previous calculations. Based on this good agreement, the optical properties were calculated and discussed in

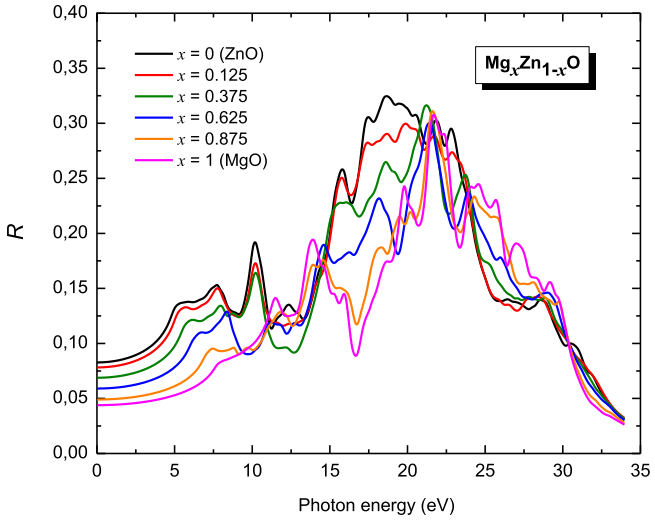

Fig. 13. Reflectivity for relaxed $Mg_xZn_{1-x}O$ alloys within the modified Becke-Johnson approach (mBJ-LDA).

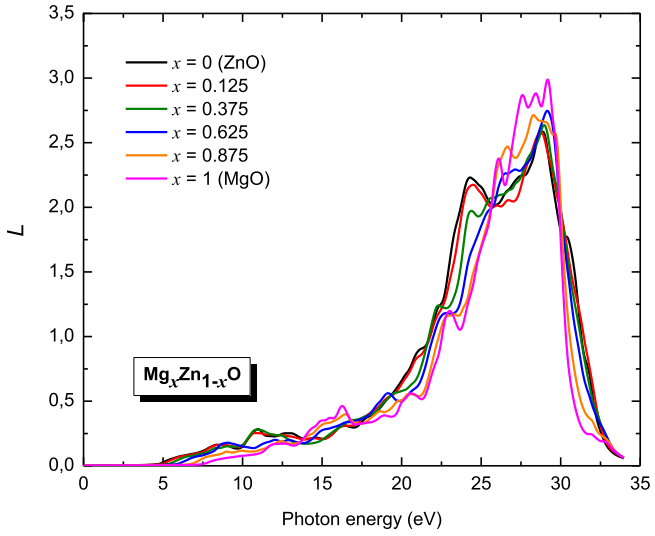

Fig. 14. Energy loss function for relaxed $Mg_xZn_{1-x}O$ alloys within the modified Becke-Johnson approach (mBJ-LDA).

details. The results signify that our studied ternary alloys are attractive materials for the optoelectronic devices area and solar cell application, in the UV region.

Acknowledgments

The author A. H. Reshak would like to acknowledge the CENTEM project, reg. no. CZ.1.05/2.1.00/03.0088, cofunded by the ERDF as part of the Ministry of Education, Youth and Sports OP RDI programme and, in the follow-up sustainability stage, supported through CENTEM PLUS (LO1402) by financial means from the Ministry of Education, Youth and Sports under the "National Sustainability Programme I. Computational resources were provided by MetaCentrum (LM2010005) and CERIT-SC (CZ.1.05/3.2.00/08.0144) infrastructures.

References

[1] W. Wei, C. Jin, J. Narayan, R.J. Narayan, J. Appl. Phys. 107 (2010) 013510.
[2] D.L. Li, Q.L. Ma, S.G. Wang, R.C.C. Ward, T. Hesjedal, X.G. Zhang, A. Kohn, E. Amsellem, G. Yang, J.L. Liu, J. Jiang, H.X. Wei, X.F. Han, Sci. Rep. 4 (2014) 7277.
[3] I.V. Maznichenko, A. Ernst, M. Bouhassoune, J. Henk, M. Däne, M. Lüders, P. Bruno, W. Hergert, I. Mertig, Z. Szotek, W.M. Temmerman, Phys. Rev. B 80 (2009) 144101.
[4] E. Diler, S. Rioual, B. Lescop, D. Thierry, B. Rouvellou, Thin Solid Films 520 (7) (2012) 2819–2823.
[5] X. Xie, Z. Zhang, B. Li, S. Wang, M. Jiang, C. Shan, D. Zhao, H. Chen, D. Shen, Opt. Express 22 (2014) 246–253.
[6] W. Yang, R.D. Vispute, S. Choopun, R.P. Sharma, T. Venkatesan, H. Shen, Appl. Phys. Lett. 78 (2001) 2787.
[7] S. Cui, W. Feng, H. Hu, Z. Feng, Y. Wang, J. Alloy Compd. 476 (2009) 306–310.
[8] A. Janotti, C.G. Van-de-Walle, Rep. Prog. Phys. 72 (2009) 126501.
[9] F.Z. Aoumeur-Benkabou, M. Ameri, A. Kadoun, K. Benkabou, Model. Numer. Simul. Mater. Sci. 2 (2012) 60–66.
[10] B. Amrani, R. Ahmed, F. El-Haj-Hassan, Comp. Mater. Sci. 40 (2007) 66–72.
[11] J.P. Perdew, S. Burke, M. Ernzerhof, Phys. Rev. Lett. 77 (1996) 3865.
[12] E. Engel, S.H. Vosko, Phys. Rev. B 47 (1993) 13164.
[13] D. Fritsch, H. Schmidt, M. Grundmann, Appl. Phys. Lett. 88 (2006) 134104.
[14] F. Tran, P. Blaha, Phys. Rev. Lett. 102 (2009) 226401.
[15] P. Blaha, K. Schwarz, G.H. Madsen, D. Kvasnicka, J. Luitz, FP-L/APW+lo Program for Calculating Crystal Properties, Vienna University of Technology, Vienna, 2001.
[16] P. Hohenberg, W. Kohn, Phys. Rev. B 136 (1964) 864–871.
[17] W. Kohn, L.J. Sham, Phys. Rev. A 140 (1965) 1133–1138.
[18] J.P. Perdew, Y. Wang, Phys. Rev. B 45 (1992) 13244.
[19] J.P. Perdew, A. Zunger, Phys. Rev. B 23 (1981) 5048.
[20] A.D. Becke, M.R. Roussel, Phys. Rev. A 39 (1989) 3761.
[21] D. Koller, F. Tran, P. Blaha, Phys. Rev. B 83 (2011) 195134–195210.
[22] D. Koller, F. Tran, P. Blaha, Phys. Rev. B 85 (2012) 155109–155118.
[23] H. Jiang, J. Chem. Phys. 138 (2013) 134115.
[24] S.D. Guo, B.G. Liu, EPL 93 (2011) 47006.
[25] S.W. Fan, L.J. Ding, Z.L. Wang, K.L. Yao, Appl. Phys. Lett. 102 (2013) 022404–022405.
[26] B.G. Yalcin, Appl. Phys. A 122 (456) (2016) 1–17.
[27] S. Bagci, B.G. Yalcin, J. Phys. D Appl. Phys. 48 (2015) 475304.
[28] B.G. Yalcin, Phys. B 462 (2015) 64–69.
[29] F.D. Murnaghan, Proc. Natl. Acad. Sci. U. S. A. 30 (1944) 244–247.
[30] H. Karzel, W. Potzel, M. Kofferlein, W. Schiessl, M. Steiner, U. Hiller, G.M. Kalvius, D.W. Mitchell, T.P. Das, P. Blaha, K. Schwarz, M.P. Pasternak, Phys. Rev. B 53 (1996) 11425–11438.
[31] J.E. Jaffe, J.A. Snyder, Z. Lin, A.C. Hess, Phys. Rev. B 62 (2000) 1660–1665.
[32] B. Amrani, I. Chiboub, S. Hiadsi, T. Benmessabih, N. Hamdadou, Solid State Commun. 137 (2006) 395–399.
[33] S. Limpijumnong, S. Jungthawan, Phys. Rev. B 70 (2004) 054104.
[34] R.S. Koster, C.M. Fang, M. Dijkstra, A. van-Blaaderen, M.A. van-Huis, J. Phys. Chem. C 119 (2015) 5648–5656.
[35] S. Desgreniers, Phys. Rev. B 58 (1998) 14102–14105.
[36] J.E. Jaffe, A.C. Hess, Phys. Rev. B 48 (1993) 7903.
[37] Y. Fei, Am. Mineral. 84 (1999) 272–276.
[38] S. Adachi, Properties of Group-IV, III–V and II–VI Semiconductors, John Wiley & Sons, England, 2005.
[39] S. Spezial, C.S. Zha, T.S. Duffy, R.J. Hemley, H.K. Mao, J. Geophys, Res. B1 106 (2001) 515–528.
[40] M.P. Habas, R. Dovesi, A. Lichanot, J. Phys. Condens. Mat. 10 (1998) 6897–6909.
[41] T. Tsuchiya, K. Kawamura, J. Chem. Phys. 114 (22) (2001) 10086–10093.
[42] A.J. Cohen, R.G. Gordon, Phys. Rev. B 14 (1976) 4593–4605.
[43] H.K. Mao, P.M. Bell, J. Geophys, Res. Solid Earth 84 (B9) (1979) 4533–4536.
[44] J.A. Sans, A. Segura, F.J. Manjón, B. Mari, A. Muñoz, M.J. Herrera-Cabrera, Microelectr. J. 36 (2005) 928–932.
[45] R.C. Whited, C.J. Flaten, W.C. Walker, Solid State Commun. 13 (1973) 1903–1905.
[46] H. Baltache, R. Khenata, M. Sahnoun, M. Driz, B. Abbar, B. Bouhafs, Phys. B 344 (2004) 334–342.
[47] V.S. Stypanyuk, A. Szasz, B.L. Grigorenko, O.V. Farberovich, A.A. Kastnelson, Phys. Stat. Sol. B 155 (1989) 179–184.
[48] K. Bougherara, F. Litimein, R. Khenata, E. Uçgun, H.Y. Ocak, Ş. Uğur, G. Uğur, A.H. Reshak, F. Soyalp, S. Bin-Omran, Sci. Adv. Mater. 5 (2013) 1–10.
[49] M.I. Ziane, Z. Bensaad, T. Ouahrani, H. Bennacer, Mat. Sci. Semicond. Proc. 30 (2015) 181–196.
[50] D.R. Penn, Phys. Rev. 128 (1962) 2093–2097.
[51] H. Bennacer, S. Berrah, A. Boukortt, M.I. Ziane, Indian J. Pure Appl. Phys. 53 (2015) 181–189.
[52] N.M. Ravindra, P. Ganapathy, J. Choi, Infrared Phys. Technol. 50 (2007) 21–29.
[53] Z. Charifi, H. Baaziz, A.H. Reshak, Phys. Stat. Sol. B 244 (9) (2007) 3154–3167.
[54] W. Martienssen, H. Warlimont, Springer Handbook of Condensed Matter and Materials Data, Springer-Verlag, Berlin, 2005.
[55] A. Schleife, C. Rödl, F. Fuchs, J. Furthmüller, F. Bechstedt, Phys. Rev. B 80 (2009) 035112.
[56] F. Wooten, Optical Properties of Solids, Academic Press, New York, 1972.